FEASIBILITY OF THERMOSYPHONS TO IMPEDE THE PROGRESS OF COASTAL PERMAFROST EROSION ALONG THE NORTHERN COASTLINE OF ALASKA

By

Jason Zottola

RECOMMENDED:

Robert Lang, Ph.D.

Hannele Zubeck, Ph.D.

Thomas Ravens, Ph.D.
Chair, Advisory Committee

Hannele Zubeck, Ph.D.
Chair, Arctic Engineering

APPROVED:

Fred Barlow, Ph.D.
Dean, College of Engineering

Date

FEASIBILITY OF THERMOSYPHONS TO IMPEDE THE PROGRESS OF COASTAL PERMAFROST EROSION ALONG THE NORTHERN COASTLINE OF ALASKA

A

PROJECT

Presented to the Faculty

of the University of Alaska Anchorage

in Partial Fulfillment of the Requirements

for the Degree of

MASTER OF SCIENCE

By

Jason Zottola, B.S.

Anchorage, Alaska

May 2016

Abstract

This study seeks to investigate the feasibility of installing thermosyphons at Drew Point, Alaska to mitigate thermally-induced coastline erosion. Portions of the northern Alaska coastline have been receding at increasing rates and putting in peril infrastructure, environmental habitats, and small villages. Slowing or eliminating the erosion would prevent emotional village relocations and costly infrastructure maintenance and relocations.

Climate and soil data from Drew Point and Barrow, Alaska are used as input variables in a numerical modeling software program to determine accurate soil thermal properties to be used in a thermosyphon design. Generalized cost considerations are presented and it is determined that thermosyphons may be an effective mitigation strategy to combat coastal erosion, however, future additional modeling could optimize a design and provide for refinements in the cost analysis.

Table of Contents

Page

List of Figures

Page

List of Tables

Page

Acknowledgments

I would like to thank Frank Urban and Gary Clow for their permission to use Drew Point, Alaska data, and for their answers to my questions. I would also like to thank Murray Fredlund from SoilVision Systems, Ltd. for permission to use modeling results from a 30-day trial of SVHeat software, and Debbie Ewanchyna of SoilVision Systems, Ltd. for being so very helpful, available, patient, and informative with respect to all my questions and concerns. And I would also like to thank the committee – Dr. Hannele Zubeck, Dr. Thomas Ravens, and Dr. Robert Lang – for their continued and patient support of my graduate studies.

Introduction and Background

Permafrost is found in most parts of Alaska with the colder, more continuous and deeper permafrost typically found in the northern half of the state (Jorgensen et al, 2008). Permafrost degradation may lead to ground subsidence, which could undermine a foundation or an embankment, leading to damage and expensive repair, maintenance or replacement (Alfaro et al, 2009). Therefore, permafrost is an important consideration in design. In most cases, the possibility of permafrost thawing is influenced by the presence of a structure placed upon it, e.g., buildings and embankments (Alfaro et al, 2009; Darrow, 2011).

However, on the coast of Alaska permafrost is thawing for environmental reasons. Thermal energy is transferred from the air and ocean water to the soil, which is warming and thawing the permafrost (Arctic Climate Impact Assessment [ACIA], 2005). Lengthened open water seasons have intensified the effects of warmer air and water temperatures and have contributed to increased coastal shoreline erosional rates over the past 50 years (Barnhart et al, 2014). This process has put structures and communities in peril and the recent trend of warming temperatures due to climate change is possibly exacerbating this problem (ACIA, 2005).

Coastal permafrost erosion may create problems to any coastal community or infrastructure that must contend with it. Problems can be social, economic and environmental in nature (Bronen, 2010). Problems include relocation, damage to structures, carbon feedback and disappearance of habitats (Gibbs and Richmond, 2015; Schaefer et al, 2012; Bronin, 2013).

Coastal erosion may force communities and villages to either find a means of preventing the erosion or to relocate. Preventing the erosion may prove prohibitively expensive, especially for small communities with little resources or remote communities with limited access to various means of transportation. Relocation is also expensive and presents challenges to the people of

the community with respect to their way of life (National Oceanic and Atmospheric Administration [NOAA], 2015).

There are many coastal oil fields with respective related infrastructure including roadway embankments, airport embankments, buildings and other such structures at or near the coast. Much of this is very expensive to construct and any preventative measures to avoid damage is paramount.

Thawing permafrost may also be linked to the disappearance of some wetlands (United States Environmental Protection Agency, 2016). Frozen soil will allow water on the surface to accumulate rather than draining downward to a water table, thereby providing a seasonal surface water body. Flora and fauna related to this environment may find fewer and fewer wetland areas if permafrost continues to thaw.

Research and investigation into the contributing factors of coastline permafrost erosion has been extensive (Ravens et al, 2012; Barnhart et al, 2014) and some modeling has been done to further investigate causes and effects (Darrow, 2011). Mitigation strategies have been proposed (NOAA, 2015), but the notion of refrigerating the frozen coastline has yet to be seriously considered, investigated and modeled. Thermosyphons have been used in other permafrost-related projects (Goering, 2003), but they have not been designed to mitigate coastal erosion.

Objective and Methodology

This project will attempt to determine the feasibility of a thermosyphon system installed on an arctic Alaska coastline, i.e. at Drew Point. The purpose of the thermosyphon system is to prevent further coastal erosion due to the seasonal heat transfer to the frozen ground at the coast.

This study will seek to determine if the installation of a thermosyphon system at Drew Point is an effective and economically feasible solution to prevent or reduce the rate of coastal permafrost erosion, and to consider if this solution could be feasible in areas where coastal permafrost erosion is affecting villages and other infrastructure.

The project is divided into four major phases: a climate data analysis, numerical modeling, a heat transfer analysis, and a thermosyphon design concept. Data is gathered from several sources and includes data from both Drew Point as well as Barrow, Alaska. Extensive data gathering includes soil parameters such as dry density, moisture content, soil type, seasonal temperature profiles, permafrost characteristics, and ground surface characteristics, and will also include climate data such as air temperature, seasonal wind speed, snowfall, winter and summer *n*-factors (air temperature multipliers for addressing the thermal effects of ground surface conditions), and a value for geothermal heat flux. Data is collected with reference to Drew Point, as well as similar locations as necessary, such as Barrow, Alaska, in order to assure a complete and thorough data set. Some data is had from previous work that involved permafrost laboratory testing and thermal modeling (de Grandpré et al, 2012). Numerical modeling is done with a finite-element software program, and a heat transfer analysis is performed using modeling results and common thermodynamics equations. Calculations, modeling and analysis is performed to determine an annual sinusoidal air temperature function, mean annual air temperature, freezing and thawing indices, frozen and unfrozen soil thermal conductivity, frozen and unfrozen volumetric specific heat, unfrozen water content as a function of temperature, seasonal trumpet curves, active layer depth, and total heat transfer.

Data Collection and Climate Analysis

Drew Point, Alaska is located on the coast of Alaska's North Slope at the Arctic Ocean, approximately 270 kilometers (167.8 miles) north of the Brooks Mountain Range. Barrow, Alaska is approximately 100 kilometers (62.1 miles) northwest of Drew Point, and just to the south of Drew Point is Teshekpuk Lake.

Due to the topography and geographic location, Drew Point experiences long, cold winters and short, cool summers. The flat, treeless terrain of the North Slope to the south and the large expanse of the Arctic Ocean to the north ensures plenty of dry, windy air at Drew Point, as is true for much of Alaska's northern coast. The sea ice that covers the Arctic Ocean in the winter ensures that the winter winds are especially dry, frigid and persistent.

Air temperature data for Drew Point was taken from the USGS site code AK100, located at Drew Point. Recording began in August 1998 and the records on the website give data recordings through July 31, 2013. The records indicate that air temperature was recorded every two hours from August 1998 through July 2003. Afterward, air temperature data was recorded every hour through July 2013, where the data set ends.

Daily air temperature averages for each day of the year were calculated by averaging all the recorded air temperatures on each day throughout the years of the data set. From the average daily temperatures, the mean annual air temperature (MAAT) was calculated as -10.8°C (12.6°F). Average daily temperatures range from approximately -32°C (-25.6°F) to 9°C (48.2°F). The freezing season starts around the end of September and lasts through the end of May, with a freezing index (FI) of 4,444 C°-days (7,999 F°-days). The thawing season provides a thawing index (TI) of 499 C°-days (898 F°-days).

A sinusoidal temperature function was developed to represent the annual air temperature curve for Drew Point, to be used in numerical analysis. A sinusoidal function is more easily employed by numerical modeling software and decreases model time. Figure 1 shows the similarity between the calculated averages and the sinusoidal function.

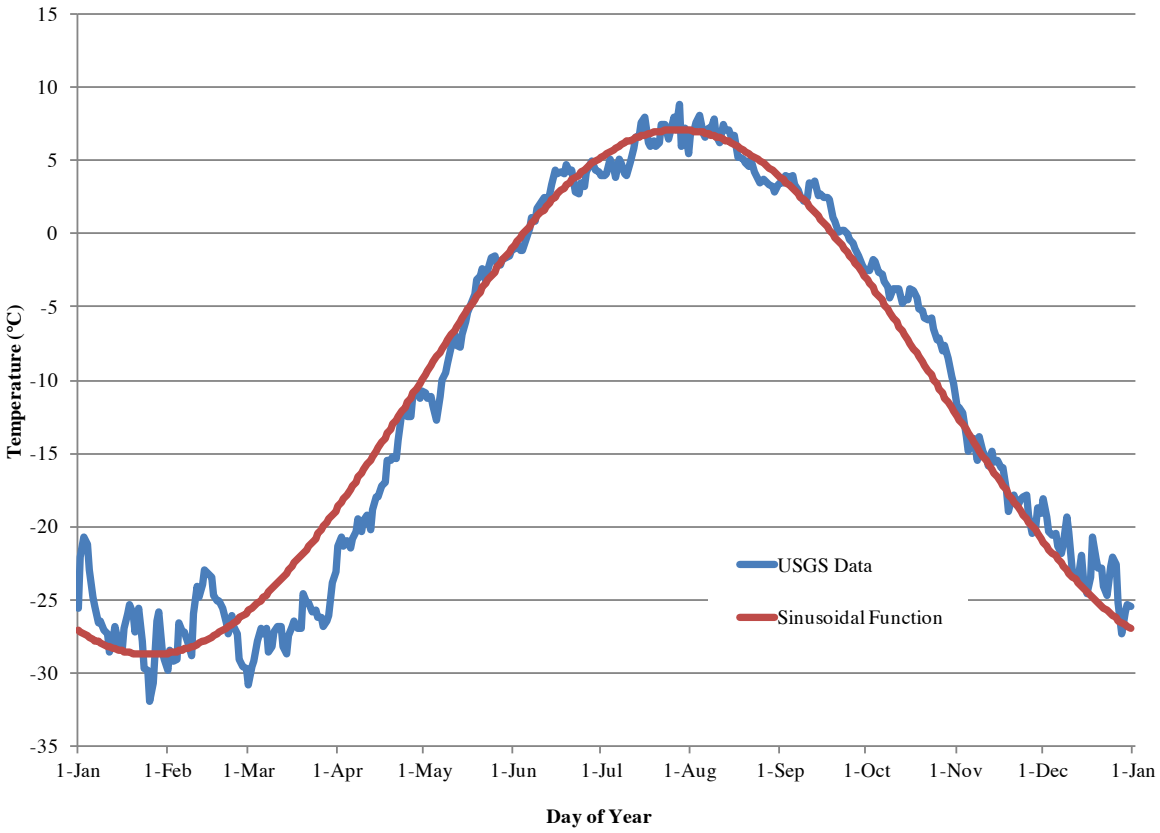

Figure 1: Drew Point Average Daily Air Temperature Data and Sinusoidal Function.

The freezing and thawing indices for the averaged temperature data closely matched the indices calculated using the sinusoidal function. The MAAT used in the sinusoidal function also matches that calculated from the raw data. These calculations further indicate that the sinusoidal function is a good representation of the annual air temperature fluctuations at Drew Point, and can be confidently used in numerical modeling. Eq. 1 and Eq. 2 show the details of the

sinusoidal air temperature function, and Table 1 compares the MAAT and the freezing and thawing indices between the data and the sinusoidal function.

$$[Eq.1] \quad T(t) = T_m - Acos\left(\frac{2\pi(t-\phi)}{365}\right)$$

where T is temperature in °C, t is day of year (January 1 is t = 1), T_m is MAAT in °C, A is the amplitude, π is pi, and ϕ is the average coldest day phase shift. Using this equation and the data for Drew Point, the following expression for temperature was developed:

$$[Eq.2] \quad T(t) = -10.81 - 17.9\cos\left(\frac{2\pi(t-26)}{365}\right)$$

Table 1: Comparison of MAAT, FI and TI

Source	MAAT (°C)	FI (C°-days)	TI (C°-days)
Average Daily Temperature Data	-10.81	4,443.51	498.54
Sinusoidal Temperature Function	-10.81	4,444.29	499.31

Near-surface temperature measurements are needed to calculate freezing and thawing *n*-factors. The Drew Point data set used above provides ground temperature measurements only as close as 5 cm (2 in.) from the surface. It is ideal to obtain ground temperature measurements as close to the surface as possible, therefore an alternate data set was used for this purpose.

The Permafrost Laboratory at the Geophysical Institute in Fairbanks, Alaska, provides data sets related to an instrumented site (Urban and Clow, 2014). The site is located between Middle Salt Lagoon and North Meadow Lake, about 4.5 kilometers (2.8 miles) northeast of the

Barrow airport, and about 2 kilometers (1.2 miles) from the coast. Polygonal ground, various small lakes, and tundra grasses and shrubs characterize this location. The Barrow and Drew Point sites are about 100 kilometers (62.1 miles) apart, at approximately the same latitude, and are both located at or very near the coast. Due to the similarities, this data set from the Barrow site was used.

The data set includes air temperature data and also includes ground temperatures at 1 cm (0.4 in.) below the ground surface. A subset of the data from September 2011 through May 2014 was used. The freezing and thawing indices for both the air temperature and the ground surface temperature were calculated for this time period. The winter *n*-factor was calculated by dividing the freezing index of the near surface by the freezing index of the air. The summer *n*-factor was calculated in the same way using the thawing indices. The winter *n*-factor was determined to be 0.68 and the summer *n*-factor was determined to be 1.08. Eq. 3 and Eq. 4 present the calculations for these parameters.

$$[Eq.\,3] \quad n_f = \frac{\Sigma FDD_{ns}}{\Sigma FDD_{air}} = \frac{8{,}592.81\ C° \cdot days}{12{,}578.74\ C° \cdot days} = 0.68$$

$$[Eq.\,4] \quad n_t = \frac{\Sigma TDD_{ns}}{\Sigma TDD_{air}} = \frac{1{,}028.80\ C° \cdot days}{948.77\ C° \cdot days} = 1.08$$

where n_f and n_t are the dimensionless freezing and thawing *n*-factors, respectively, FDD_{ns} and FDD_{air} are the cumulative freezing degree-days for the period for near-surface temperature and air temperature, respectively, and TDD_{ns} and TDD_{air} are the cumulative thawing degree-days for the period for near-surface temperature and air temperature, respectively.

An *n*-factored sinusoidal function was developed (Eq. 5), which can be seen along with the first sinusoidal function and the averaged daily temperature data curve, in Figure 2. The *n*-factored freezing and thawing indices are 3,022 C°-days (5,440 F°-days) and 539 C°-days (970 F°-days), respectively.

$$[Eq.5] \quad T(t) = -6.8 - 13.5cos\left(\frac{2\pi(t-26)}{365}\right)$$

where T is temperature in °C, and t is day of year (January 1 is t = 1).

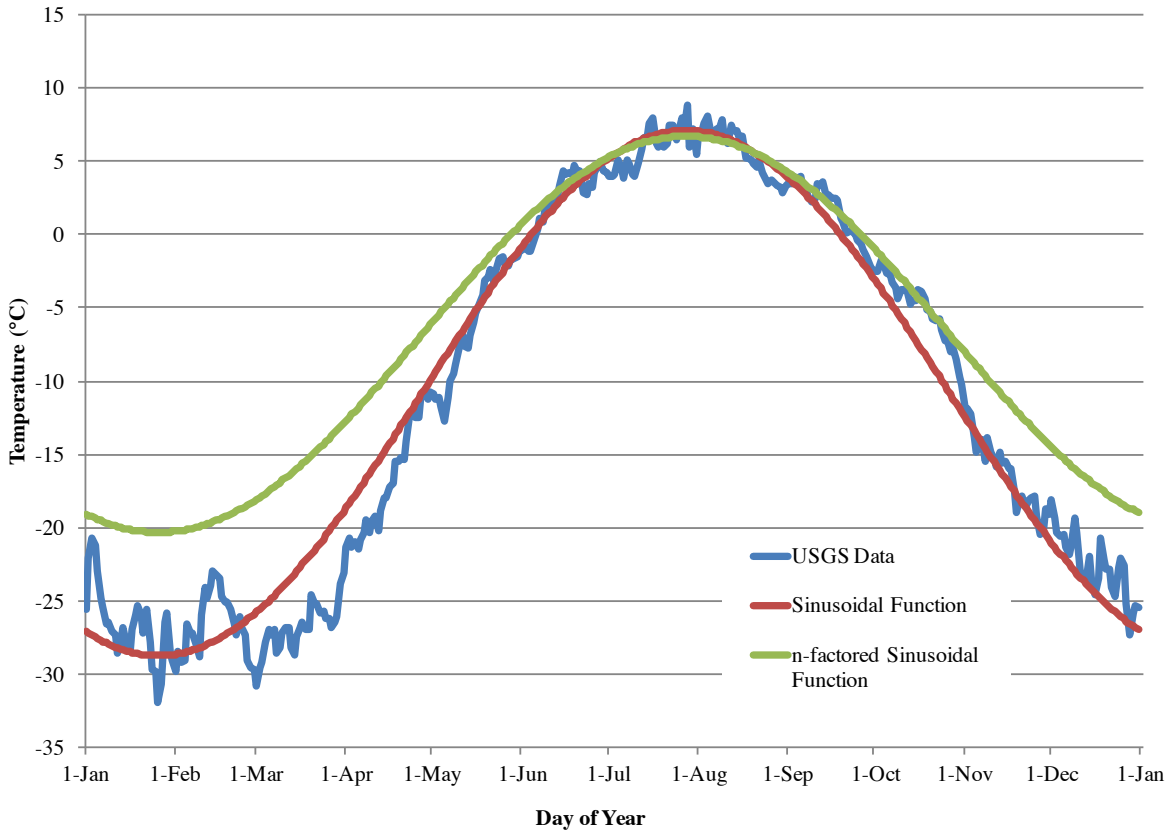

Figure 2: *n*-factored Sinusoidal Air Temperature Function for Drew Point.

Rain and snowfall data is minimal in the Drew Point data set and could not be found for the Barrow 2 instrumented site, so a third data set was used to gather information on precipitation. The Western Regional Climate Center (WRCC) provides climate data from Station 500546, located at the Barrow, Alaska airport. Average daily climate values are provided for the period 1949 to 2005.

The climate station receives an annual average of 11.5 cm (4.5 in.) of rainfall and approximately 74 cm (29.1 in.) of average annual snowfall. Snow generally covers the ground from the beginning of September through mid-June. The average snow depth is approximately 20 cm (7.9 in.) and the maximum average snow depth is about 30 cm (11.8 in.) and occurs around the first of April. Snowfall depths increase rapidly at the beginning of the snowfall season in late September through November, and then slowly and steadily increases through to the spring thaw season.

The Drew Point data set has ample wind data with respect to both speed and direction, though in this study the direction of the wind is not important. An analysis of the data indicates the average annual wind speed at Drew Point is 4.4 m/s (9.8 mph). Figure 3 illustrates the average daily wind speed throughout the year. From the figure, it is clear the average wind speed does not change too much throughout the year. There are no lengthy periods of notable significant higher or lower wind speeds.

However, because wind speed is critical to the operation of thermosyphons (discussed in detail later), the average daily wind data was separated into two categories: days when the average daily air temperature is below 0°C (32°F), and days when the average daily air temperature is above 0°C (32°F). Each was analyzed separately to determine if there was any noticeable, and important, average difference between “cold” and “warm” days. The average

wind speed on "warm" days was found to be 4.2 m/s (9.4 mph), while on "cold" days it was 4.5 m/s (10.1 mph). The difference is small, but is significant enough to consider when conducting a heat transfer analysis for a thermosyphon system, which generally only operates during cold ambient air conditions.

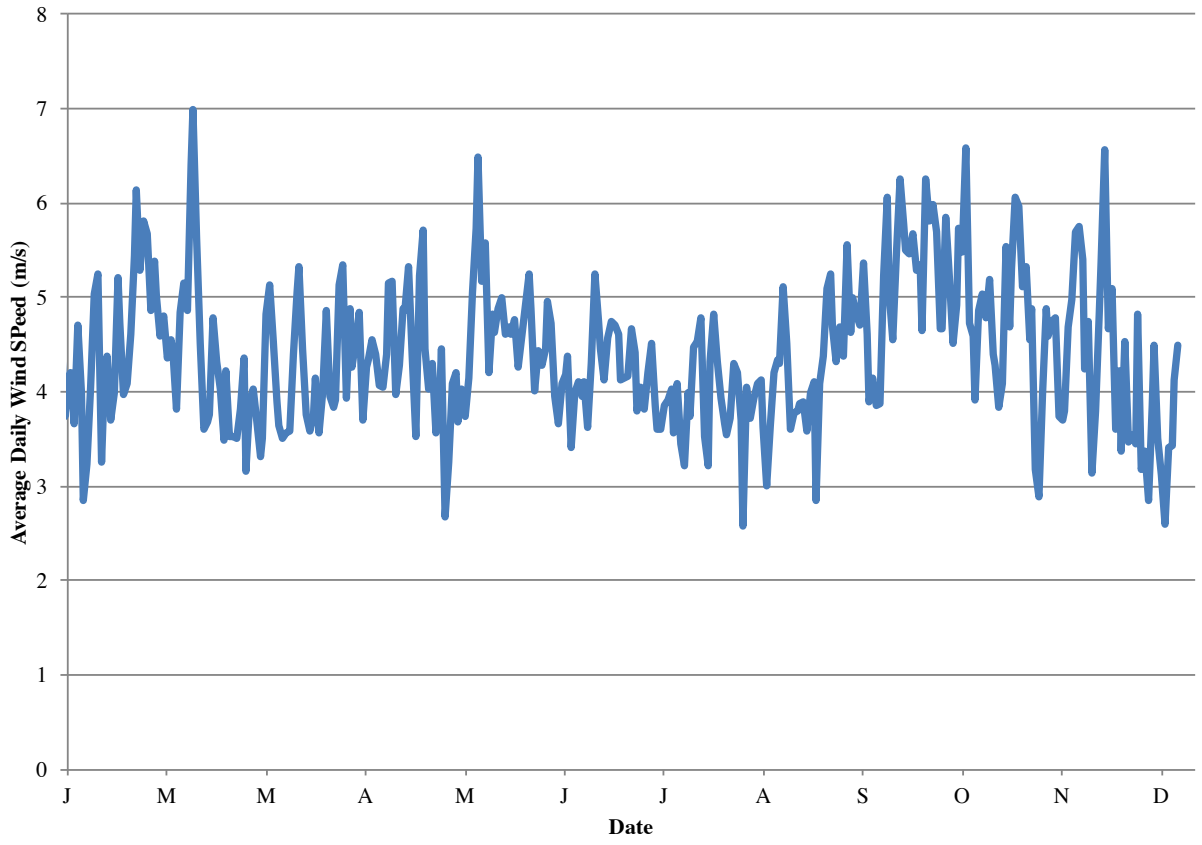

Figure 3: Average Daily Wind Speed at Drew Point

Drew Point is in the continuous permafrost zone (Jorgensen et al, 2008). The permafrost is present to a depth of 324 meters (1,063 feet) below the ground surface (National Snow and Ice Data Center, 1998), and is comprised of cold, ice-rich, fine-grained material near the surface (Barnhart et al, 2014). Data from Drew Point and Barrow indicate the average annual permafrost

temperature is approximately -8.5°C (16.7°F) to -5.5°C (22.1°F) through the upper 15 meters (49.2 feet). The average soil temperature was calculated and graphed as a trumpet curve (Figure 4). The curve reveals the active layer to average approximately 45-50 cm (17.7-19.7 in.). This is in good agreement with data from Drew Point as illustrated in Figure 5.

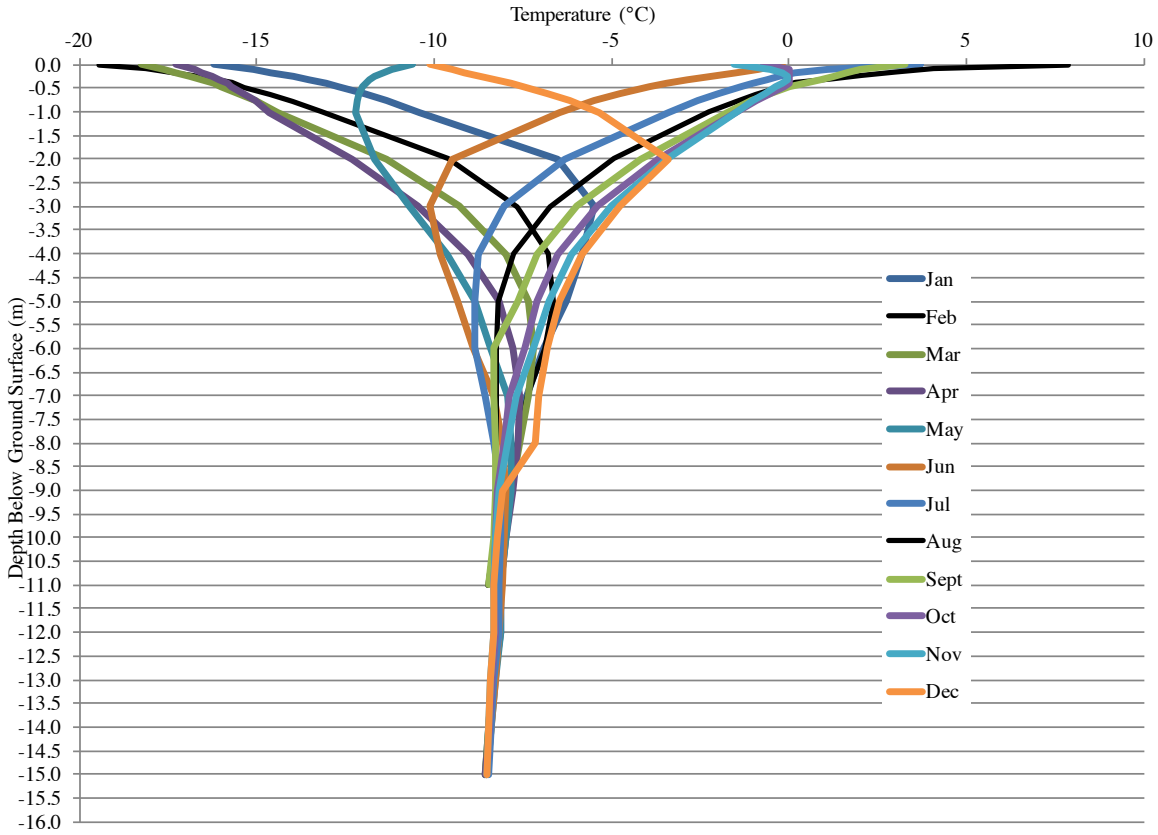

Figure 4: Trumpet Curve for Barrow Data (2011-2014)

Modeling

SVOffice™ 5, a finite-element software program developed by SoilVision Systems, Ltd, was used to create two models of the bluffs at Drew Point. Modeling was performed for two reasons: to confirm the validity of assuming air temperature and soil temperature similarities

between Drew Point and Barrow, and to provide accurate values for heat transfer calculations and thermosyphon design. The data at Barrow provided soil temperatures to a depth of 15 meters (49.2 feet) so the two-dimensional model (Model A) that was developed used this same depth. The soil types used were peat and silt, the former comprising the upper 30 cm (11.8 in.) while the latter comprising the remainder of the 15-meter depth.

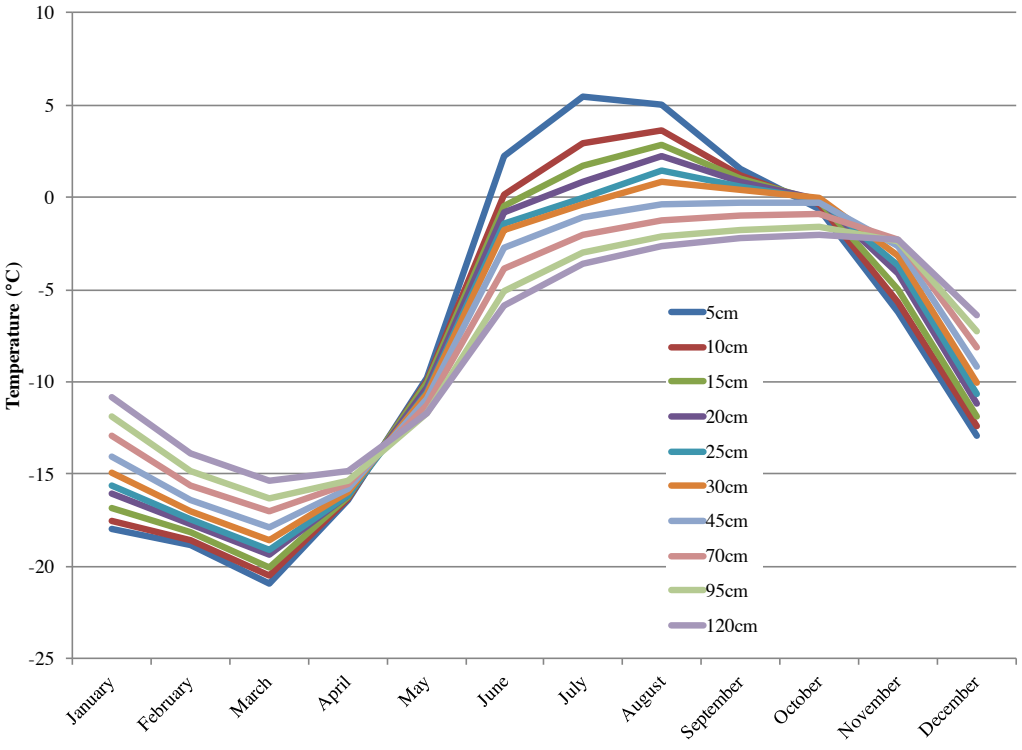

Figure 5: Annual Average Temperature for Various Depths, Drew Point (2003-2013).

The following equations from Slusarchuk and Watson (1975) can be used to calculate frozen and unfrozen thermal conductivity of silt:

$$[Eq.6] \quad K_f = 0.0058\rho_{ds} + 0.74$$

$$[Eq.7] \quad K_u = 0.0101\rho_{ds} - 0.14$$

where K_f and K_u are frozen and unfrozen thermal conductivity, respectively, in W/m·K, and ρ_{ds} is soil dry density in kg/m^3. And the following equations from the Joint Departments of the Army and Air Force, USA (1988) can be used to calculate frozen and unfrozen volumetric specific heat of silt:

$$[Eq.8] \quad C_f = \rho_{ds}\left(0.17 + 0.5\frac{W}{100}\right)$$

$$[Eq.9] \quad C_u = \rho_{ds}\left(0.17 + 1.0\frac{W}{100}\right)$$

where C_f and C_u are frozen and unfrozen volumetric specific heat, respectively, in Btu/ft^3·°F, ρ_{ds} is soil dry density in lbs/ft^3, and W is water content in percent.

Eq. 6 through Eq. 9 were converted into Eq. 10 through Eq. 13, respectively, to accommodate SI units for input variables and to provide SI units for the results. The equations used to calculate frozen and unfrozen thermal conductivity:

$$[Eq.10] \quad K_f = 0.000625\rho_{ds} + 1.28$$

$$[Eq.11] \quad K_u = 0.001089\rho_{ds} - 0.242$$

where K_f and K_u are frozen and unfrozen thermal conductivity, respectively, in W/m·K, and ρ_{ds} is soil dry density in kg/m^3. And the equations used to calculate frozen and unfrozen volumetric specific heat:

$$[Eq.\,12] \quad C_f = 4.17\rho_{ds}\left(0.17 + 0.5\frac{W}{100}\right)$$

$$[Eq.\,13] \quad C_u = 4.17\rho_{ds}\left(0.17 + 1.0\frac{W}{100}\right)$$

where C_f and C_u are frozen and unfrozen volumetric specific heat, respectively, in kJ/m^3·K, ρ_{ds} is soil dry density in kg/m^3, and W is water content in percent.

The volumetric water content of the soils at Drew Point has a wide range of values. The water content is "typically greater than 30%" (Barnhart et al, 2014), and as high as 80% (Jorgensen and Brown, 2005). The large ice wedges located at the site (Barnhart et al, 2014; Ravens et al, 2012) likely provide a significant contribution to the water content.

Using a 50% volumetric water content and a soil dry density of 1,200 kg/m^3 (74.8 lb/ft^3) (Barnhart et al, 2014), the values for frozen and unfrozen thermal conductivity of silt are 2.03 W/m·K (1.17 Btu/hr·ft·°F) and 1.06 W/m·K (0.61 Btu/hr·ft·°F), respectively, and the values for frozen and unfrozen volumetric specific heat of silt are 2,102 kJ/m^3·K (31.37 Btu/ft^3·°F) and 3,353 kJ/m^3·K (50.04 Btu/ft^3·°F), respectively. Values for the same soil parameters were determined for peat using values from de Grandpré et al (2012): 750 kg/m^3 (46.8 lbs/ft^3) for dry density, 1.02 W/m·K (0.59 Btu/hr·ft·°F) for frozen thermal conductivity, 0.38 W/m·K (0.22 Btu/hr·ft·°F) for unfrozen thermal conductivity, 1,380 kJ/m^3·K (20.59 Btu/ft^3·°F) for frozen

volumetric specific heat, and 2,625 kJ/m^3·K (39.17 Btu/ft^3·°F) for unfrozen volumetric specific heat.

Unfrozen water content, W_u, was determined using the following equation from Anderson and Tice (1972):

$$[Eq.14] \quad W_u = m\Theta^n$$

where Θ is the number of degrees below 0°C, expressed as a positive number and m and n are empirical parameters. For Fairbanks silt, Anderson and Tice give values for m and n of 4.81 and -0.33, respectively.

The n-factored sinusoidal temperature function (Eq. 5) was used as an upper boundary condition to represent the ambient air temperature fluctuations at the ground surface. Using a geothermal heat flux map (Batir et al, 2015) a geothermal heat flux value of 70 mW/m^2 (0.022 Btu/hr·ft^2) was applied to the lower boundary of the model. Calculations using data from Drew Point and Barrow indicated the average annual soil temperature to be about -7°C (19.4°F) and this value was used an initial condition for both the peat and silt.

Temperature was recorded with time at eight different depths within 1 m (3.28 ft) of the surface, and at every meter of depth from 1 m to 15 m (3.28 ft to 49.2 ft) to parallel the soil temperature data depths from Barrow. The model was run for 100 years to ensure that stabilized annual temperature oscillations would be observed within the soil at all depths.

The initial conditions and the boundary conditions of the model were very good selections as the soil temperatures did not change much by the 100th year. The annual soil temperatures with depth generally stabilized within the first 15-20 years. The deepest soil

temperatures took longer, however, even the deepest soils at 15 meters (49.2 ft) had stabilized in under 40 years. And these temperature stabilizations were only a few tenths of a degree Celsius from the -7°C temperature given as an initial condition.

The coastal permafrost at Drew Point also has a vertical "surface" component as there is exposed frozen, ice-rich silt that experiences the same climatic air temperature conditions as the horizontal ground surface, which is covered in a modeled 30 cm (11.8 in) of peat. The exposed vertical surface does not have an insulating layer of peat to protect the frozen soil and so a new sinusoidal temperature function, using new summer and winter *n*-factors, was needed to model the heat transfer through this vertical surface, which Model A did not consider.

A second model (Model B) was run with all the same variables and geometry as the first model, with the exception of two differences: a new sinusoidal temperature function (Eq. 15) was calculated using a summer *n*-factor of 2.0 and a winter *n*-factor of 0.9 (Zarling, 2011), and the layer of peat was removed and replaced with silt.

$$[Eq.\,15] \quad T(t) = -8.2 - 19.5\cos\left(\frac{2\pi(t-26)}{365}\right)$$

where T is temperature in °C, and t is day of year (January 1 is t = 1).

Annual soil temperature oscillations stabilized once again at all depths, well before the end of the 100-year model run. The results and data from both 2-D models were then tabulated and organized for use in a heat transfer analysis.

Heat Transfer Analysis

The numerical modeling analysis considered heat transfer into the soil through the horizontal ground surface, through the vertical bluff face, and through geothermal heat flux. The annual temperature fluctuations in the soil due to these heat transfer sources reached an annual equilibrium sine wave between the maximum and minimum temperatures. This equilibrium was observed after approximately 20-30 years of modeled time.

The difference between the annual maximum and minimum soil temperatures were used to calculate the difference in the amount of heat in the soil on a per-volume basis. The thermosyphons are planned to be spaced 3 meters (9.84 ft) apart, center-to-center, and so the volume of soil considered for the calculations was a cylinder with a height equal to the embedment length, i.e. five meters (16.4 ft), and a radius of 1.5 meters (4.92 ft) – half of the spacing distance. Also included in the volume was a hemisphere with a radius of 1.5 meters (4.92 ft) to account for the soil affected by the thermosyphon evaporator tip.

Following the modeling, the heat transfer was calculated in two phases using the results of the respective models. The first heat transfer calculation was done using the modeling results from Model A, which considered the heat transfer to the soil through the horizontal ground surface. The cylinder of soil was considered in parts equal to smaller, or "shorter", cylinders. The first had a height equal to the depth of peat, i.e. 0.3 meters (0.98 ft). The next cylinder was given a height of 0.2 meters (0.66 ft), the third a height of 0.5 meters (1.64 ft). The remaining cylinders were given heights of one meter, down to the 5-meter (16.4-ft) embedment depth. The volume of each cylinder was then calculated and the difference between the annual maximum and minimum temperatures within each cylinder was then calculated. Using the volume and the temperature differences, the total heat transfer was calculated using the frozen and unfrozen

volumetric specific heats. Volumetric specific heat values for silt were calculated using Eq. 8 and Eq. 9. In addition, the latent heat of fusion of water had to be considered and calculated in any peat and silt layers that experienced an annual freeze/thaw cycle. The total heat transfer in each layer was calculated and totaled. The hemisphere portion of soil was also considered and given the thermal values used in the bottommost layer of the cylinder, i.e. the layer between 4 meters (13.1 ft) and 5 meters (16.4 ft) below the ground surface.

The results from Model B, which considered heat transfer through the vertical bluff face, were then calculated in the same manner – with two differences: (1) the bluff face does not have a layer of peat at the surface and therefore all calculated soil layers only considered silt, and (2) the layers were calculated in vertical slices of a cylinder and hemisphere. These heat transfer totals were then added to the total from Model A. This represented the total difference in the amount of heat present in the ground between the warmest and coolest times of the year. Table 2 and Table 3 include the layer-by-layer tabulated calculations. The total thermal energy difference was 4,627,205 kJ (4,385,976 Btu) per season.

Thermosyphon Design

The type of thermosyphon used for this study is called a two-phase thermosyphon. A two-phase thermosyphon uses a working fluid to passively transfer heat. Heat is transferred to the liquid, which then boils. This gas phase transports the heat to the condenser where it releases the heat, returns to a liquid and falls back to the evaporator. This cycle will continue while the air temperature remains below that of the soil temperature. Thermosyphons are able to freeze thawed or otherwise unfrozen ground as well as maintain frozen ground. A frozen area of

ground is useful for foundation stability and essentially any situation where frozen ground is necessary.

Table 2: Heat Transfer Analysis – Model A

Material	Depth (m)	Height (m)	Avg. Annual Min. Temp. (°C)	Avg. Annual Max. Temp. (°C)	Volume (m^3)	Unfrozen Volumetric Specific Heat (kJ/m^3 K)	Frozen Volumetric Specific Heat (kJ/m^3 K)	Volume of Water (m^3)	Thermal Energy Difference (kJ)
Peat	0 - 0.3	0.3	-18.60	3.93	2.12	2,625	1,380	1.06	430,443
Silt	0.3 - 0.5	0.2	-17.50	1.25	1.41	3,353	2,102	0.71	294,019
Silt	0.5 - 1.0	0.5	-15.20	-1.26	3.53	n/a	2,102	n/a	103,561
Silt	1.0 - 2.0	1.0	-13.48	-3.60	7.07	n/a	2,102	n/a	146,799
Silt	2.0 - 3.0	1.0	-11.40	-5.84	7.07	n/a	2,102	n/a	82,611
Silt	3.0 - 4.0	1.0	-9.77	-7.26	7.07	n/a	2,102	n/a	37,294
Silt	4.0 - 5.0	1.0	-8.61	-7.99	7.07	n/a	2,102	n/a	9,212
Silt	Hemisphere	1.5	-8.61	-7.99	7.07	n/a	2,102	n/a	9,212

Table 3: Heat Transfer Analysis – Model B

Material	Depth (m)	Height (m)	Avg. Annual Min. Temp. (°C)	Avg. Annual Max. Temp. (°C)	Volume (m^3)	Unfrozen Volumetric Specific Heat (kJ/m^3 K)	Frozen Volumetric Specific Heat (kJ/m^3 K)	Volume of Water (m^3)	Thermal Energy Difference (kJ)
Silt	0 - 0.5	0.5	-25.00	8.00	4.26	3,353	2,102	2.13	1,049,553
Silt	0.5 - 1.0	0.5	-22.00	4.00	7.63	3,353	2,102	3.82	1,729,385
Silt	1.0 - 1.5	0.5	-18.25	0.00	9.30	n/a	2,102	n/a	356,762
Silt	1.5 - 2.0	0.5	-14.70	-3.25	9.30	n/a	2,102	n/a	223,831
Silt	2.0 - 2.5	0.5	-12.50	-5.35	7.63	n/a	2,102	n/a	114,674
Silt	2.5 - 3.0	0.5	-11.05	-6.60	4.26	n/a	2,102	n/a	39,848

Doubling the "cooling capacity" of winter will provide for lower soil temperatures in the spring and a larger sink for summer heat. Each thermosyphon must provide 4,627,205 kJ (4,385,976 Btu) of cooling per season. Average annual daily temperatures in Drew Point provide a cooling season of 253 days, therefore each thermosyphon must transfer approximately 762 kJ/hr (722 Btu/hr), on average, during the length of the winter season.

The basic heat transfer equation will be used:

$$[Eq.16] \quad q = \frac{\Delta T}{R}$$

where q is heat in W, T is temperature in °C, and R is resistance in °C/W.

The average winter soil temperature is -7°C (19.4°F) and average winter air temperature is -17.5°C (0.5°F), therefore ΔT is 10.5°C (18.9°F). The total thermal resistance is the radial resistance from the outer edge of the radius of the aforementioned cylinder to the thermosyphon evaporator wall (for each soil layer), the hemispherical resistance at the tip of the evaporator, and the radiator resistance. The soil resistances act in parallel with each other, and together act in series with the radiator resistance. Eq. 17, Eq. 18 and Eq. 19 (American Society of Heating, Refrigerating and Air Conditioning Engineers [ASHRAE], 2001) were used to find the total resistance in the soil.

$$[Eq.17] \quad R_{radial} = \frac{ln\frac{r_o}{r_i}}{2\pi kH}$$

$$[Eq.18] \quad R_{hemispherical} = \frac{\frac{1}{r_i} - \frac{1}{r_o}}{2\pi k}$$

where R is resistance in °C/W, r_o is the outer radius in meters, r_i is the inner radius in meters, k is the thermal conductivity of the material in W/m·K, and H is the thickness of the soil layer in meters. In this case, there were three terms of soil resistance: a layer of peat, a layer of silt, and

the silty hemispherical portion. The three terms of resistance were combined as in Eq. 19 (ASHRAE, 2001):

$$[Eq.19] \quad R_{soil} = \frac{1}{\frac{1}{R_{peat}} + \frac{1}{R_{silt}} + \frac{1}{R_{hemispherical}}}$$

The conductance of the thermosyphon is expressed in Imperial units according to Eq. 20 (Wagner, 2014), and is the reciprocal of its resistance.

$$[Eq.20] = \ C = Aeh = \frac{1}{R_{radiator}}$$

where C is the radiator conductance in Btu/hr·°F, A is the radiator surface area in ft^2, e is a unitless variable for fin efficiency, h is the surface heat transfer coefficient in Btu/hr·ft^2, and $R_{radiator}$ is the radiator resistance in hr·°F/Btu.

The surface of the area may be selected by the designer or manufacturer, however, standard sizes are more cost-effective to produce and for this study a 170-ft^2 radiator will be used. The surface heat transfer coefficient, h, is calculated using wind speed using Eq. 21 (Johnson, 1971), and the fin efficiency, e, is a function of the surface heat transfer coefficient, the thermal conductivity of the radiator material, and the dimensions of the radiator fins.

$$[Eq.21] \quad h = 0.69 + 1.23V^{0.42}$$

where h is the surface heat transfer coefficient in Btu/hr·ft^2 and V is wind speed in miles per hour. As indicated earlier, the average winter wind speed at Drew Point is 4.5 m/s, or 10.1 miles per hour, which when used in Eq. 21 gives a surface heat transfer coefficient of 3.94 Btu/hr·ft^2 (12.4 W/m^2).

The 2001 ASHRAE Fundamentals Handbook (ASHRAE, 2001) provides a chart to determine fin efficiency values for annular fins of constant thickness using two calculated values given by Eq. 22 and Eq. 23:

$$[Eq.22] \quad \frac{X_e}{X_b}$$

where X_e is the radial distance to the outer edge of the radiator fins, X_b is the radial distance to the outside surface of the inner radiator pipe (or base of the radiator fins).

$$[Eq.23] \quad W\sqrt{\frac{h}{ky_b}}$$

where W is the radial length of the fins, h is the surface heat transfer coefficient, k is the thermal conductivity of the fin material, and y_b is fin thickness.

Using Eq. 22 and Eq. 23 and Figure 16 (ASHRAE, 2001), fin efficiency, e, is approximately 0.92. Inserting this result into Eq. 20, along with the result from Eq. 21, the thermosyphon conductance is calculated to be 616.1 Btu/hr·°F (325 W/°C). The radiator resistance is then 0.00162 hr·°F/Btu (0.00377 °C/W).

Using the values for soil resistance and radiator resistance, the difference in average soil temperature and air temperature, and Eq. 16, a total heat transfer is calculated as 223.5 W (762.7 Btu/hr), which converts to 804.8 kJ/hr, which is greater than the 762 kJ/hr (722 Btu/hr) required to double the "cooling capacity" of winter.

The 170-ft^2 radiator, or condenser, is made of carbon steel with 15.2-cm (6-in) outside diameter fins and an 8.9-cm (3.5-in) outside diameter pipe. The condenser is welded to a steel pipe evaporator with an 8.9-cm (3.5-in) outside diameter. The evaporator pipe extends 5 meters (16.4 feet) vertically below the ground surface. The thermosyphon is fitted with a lift ring for installation purposes and a charging valve. Fabrication includes welding the thermosyphon components together, testing the welds using non-destructive examination such as pneumatic testing and magnetic particle procedures. Upon passing all testing, the thermosyphon condenser and evaporator is then coated to prevent corrosion. The condenser is also painted white to maximize solar reflection and emissivity. The thermosyphon is then charged for heat transfer.

Discussion

Equally important as the effectiveness of a thermosyphon system to mitigate coastal erosion is the costs of such a project. The cost of this project would likely be most useful as a cost-per-distance basis, e.g. the cost per kilometer of installing such a system at Drew Point, Alaska. The thermosyphon unit described earlier would likely cost approximately several thousand dollars. Using a 3-meter (9.84 ft) spacing, approximately 333 thermosyphons would be needed for each kilometer (0.61 mi) of coastline protection.

However, manufacturing is only one component of the total cost. Costs associated with shipping, installation, safety and maintenance must also be considered. Shipping to a location

that is not on the road system would require more effort and expense than that needed for simply loading a truck, driving the material to a destination, and unloading the truck. This project would require loading a truck in Anchorage and hauling the load (likely many loads) to Deadhorse, Alaska. One option for further transportation after Deadhorse is described in a Bureau of Land Management Contract No. L09PC00243 (U.S. Department of the Interior, 2009). In this proposal, equipment and materials are transported overland to Oliktok Point where it is transferred to a cat-train for transportation over tundra and sea ice through the Colville River Delta, Kogru River, Lonely, and then to Drew Point. Air transport is provided by fixed-wing aircraft landing on the grounded ice north of Drew Point to support mobilization. Cost, and the logistics of seasonal timing, would likely add significantly to the cost of this project.

Installation of the thermosyphons includes mobilization of drilling and lifting equipment, as well as man-camps that include living supplies for multiple teams of labor and support personnel. Each thermosyphon would need to be lifted into the air and lowered into a borehole in the permafrost.

Safety with respect to life and bodily injury, as well as the protection of equipment, all must be considered. Staging a project of this magnitude along a rapidly degrading coastline provides a few safety challenges. The most important is the safety of the crews working at the site. Firm ground would need to be located to provide crews with a safe platform to assist with the unloading of aircraft and cat-trains, a location to erect man-camps, and a place to initiate drilling. Heavy equipment and human life would both be best kept at a distance from the shoreline as much as possible and, in fact, the project itself would need to be installed at a distance from the coastline that would allow for the safe completion of the project without crews or equipment having to risk the hazards associated with an eroding coastline approaching the

project location. Thermosyphons would be installed several hundred meters from the coastline. Over time the eroding coastline would retreat toward the thermosyphons. The thermosyphons would then counteract the effects of thermal erosion and the rates of coastline retreat would decrease or cease.

Maintenance is really only a very small cost consideration as passively operating thermosyphons do not require human operation or intervention. The only costs associated with thermosyphon maintenance would be the advised periodic operation inspection. An inspection such as this would include a multi-person crew to travel to the site to measure the internal pressure and contact temperature of each thermosyphon. These measurements will allow the crew to determine the operational status of each thermosyphon to ensure its continued effectiveness. These data also allow for the calculation of the soil temperature at the lowermost portion of the thermosyphon evaporator. This work entails only a few minutes at each thermosyphon so a two-person crew would be able to gather data from several hundred thermosyphons each day. A thermosyphon with an inadequate pressure or temperature measurement would need further maintenance, which would likely consist of recharging the unit with working fluid after an inspection of the integrity of the charging valve and above-grade welds. Maintenance is minimal and failed thermosyphons are rare so the cost of continued long-term thermosyphon operation at Drew Point is minimal and would be dwarfed by the initial expense of manufacturing and installation. Thermosyphons are installed at locations throughout Alaska and many have been operating for several decades with no need for repair or replacement.

The climate analysis, preliminary modeling results and thermosyphon design from this project could serve as a starting point for future research. Two significant areas of research,

which are related and intertwined, are the cost analysis considerations and further numerical modeling. Research into the costs associated with shipping, mobilization and installation would add dramatically to the initial costs of manufacturing. Shipping, mobilization and installation at Drew Point is complicated by the fact that Drew Point is not on the road system and would require some creative, and possibly very expensive, methods of shipping and mobilization. And the installation would be complicated by the safety considerations associated with working on a ground surface that is eroding and retreating.

Further numerical modeling would allow a study into several areas of likely interest related to a thermosyphon project at Drew Point. A thermosyphon could be added to the models described in this project, which would allow for an investigation and study into the effectiveness of the thermosyphon with respect to thermal considerations and erosional rates. A numerical model that includes a component to study the mechanical erosion effects of wave action at the Drew Point coastline could be coupled with the thermal analysis. Though thermosyphons provide thermal support in the form of lowering the soil temperature (and therefore increasing soil adfreeze strength), they do not, in this project, provide increased structural support to the coastal bluffs.

Numerical modeling could also support an in-depth sensitivity analysis and optimization design study. A well-developed modeling program could study the effectiveness of various parameters of a thermosyphon design such as the embedment depth, condenser fin area and thermosyphon spacing. Decreased embedment depth, decreased condenser fin area and increased thermosyphon spacing would all support decreased manufacturing costs, however would also decrease the cooling effects to the soil. A sensitivity analysis involving these variables could seek to optimize a thermosyphon design based on the cooling effects and costs

associated with each variable. It's possible, for example, that increasing the condenser fin area would allow for an increased thermosyphon spacing. If so, the reduction in the number of thermosyphon units needed could offset the increased unit costs associated with manufacturing, transportation and installation.

Another important consideration related to a thermosyphon project at Drew Point is the possibility of using an alternate type or style of thermosyphon – a hybrid thermosyphon. A hybrid thermosyphon provides both passive and active cooling. Passive cooling is had using the design described in this project, i.e., using a working fluid to passively transfer heat from the soil to the air when the air temperature is lower than the soil temperature, which is a winter season process. It is possible that modeling may prove that a mitigation strategy that also includes cooling throughout the summer season would be needed. If so, a hybrid thermosyphon could be designed that would provide active cooling any time air and soil temperatures do not allow for passive operation. Active refrigeration of the soil would increase manufacturing costs and would also increase maintenance and repair costs so a new cost analysis would also need to be completed.

Conclusion

This study has analyzed and summarized soil and climate data for Drew Point, Alaska. The analysis has been used to develop a preliminary numerical model of the bluffs located at Drew Point. Input parameters and modeling results have been used to design a preliminary mitigation strategy to counteract coastal erosion using thermosyphons to provide an increased cooling of the soil.

The thermosyphon described in this study would more than double the "cooling capacity" of the Drew Point winter season, therefore decreasing soil temperatures. The design described is one of a myriad of possibilities. Thermosyphons may be custom designed and manufactured to incorporate project-specific demands with respect to evaporator embedment and radiator conductance. Variations on the thermosyphon design would alter the costs associated with manufacturing, and would also alter the transportation and installation costs if the number of thermosyphon units needed would be increased or decreased. A well-developed modeling study would be useful in studying the effects of thermosyphon variables on the effectiveness of coastal erosion mitigation and would also be useful for design and cost optimization.

Decreasing or halting the retreat of the northern coastline of Alaska could provide the protection needed to oil production facilities, military sites and coastal villages, as well as provide an option for environmental protection, as halting the retreat of the coastline toward a freshwater lake would allow for the protection of the lake from saltwater intrusion due to an advancement of the ocean toward the lake. Refrigerating the coastline by reducing soil temperatures through the cooling capacity of thermosyphons provides one option toward these objectives.

The long-term effectiveness of a thermosyphon-related project to refrigerate the coastline is only limited by the service life of the thermosyphon and the capability of the thermosyphon to reduce or eliminate the rate of coastline retreat. Two-phase passive thermosyphons have little to no maintenance costs associated with them and rarely need to be serviced, repaired or replaced. Thermosyphons that are decades old are still operating in Alaska and providing subgrade cooling to various projects and infrastructure. The reduction in the rate of coastline retreat would likely be the controlling factor in determining how long a mitigation strategy such as this would

provide protection. If thermosyphons can provide an additional several decades of protection from coastal retreat to an environmental site, a village, military sites, and expensive oil infrastructure, then perhaps the cost of such a strategy can be justified. A village has financial, environmental, social and emotional value; an environmental site once gone cannot be replaced; a military site provides needed protection; and infrastructure related to oil is not only is expensive but provides much toward the state and national economy. All of these are valuable resources and all of these are important reasons to consider the mitigation of coastline erosion and retreat. Refrigeration of the coastline through a thermosyphon strategy may be a feasible option for these various entities.

References

ACIA, 2005. Arctic Climate Impact Assessment. Cambridge University Press, 1042p.

Alfaro, M., Ciro, G., Thiessen, K., Ng, T. (2009). Case Study of Degrading Permafrost beneath a Road Embankment. *Journal of Cold Regions Engineering, 23*(3), p. 93-111.

American Society of Heating, Refrigerating and Air Conditioning Engineers, Inc. (2001). *ASHRAE HVAC Fundamentals Handbook*, Atlanta, GA.

Anderson, D. M., Tice, A. R. (1972). Predicting Unfrozen Water Contents in Frozen Soils from Surface Area Measurements. *Highway Research Record*, (393).

Barnhart, K. R., R. S. Anderson, I. Overeem, C. Wobus, G. D. Clow, F. E. Urban. (2014). Modeling erosion of ice-rich permafrost bluffs along the Alaskan Beaufort Sea coast. *Journal of Geophysical Research: Earth Surface, 119*, doi: 10.1002/2013JF002845.

Batir, J., Blackwell, D., and Richards, M. (2015). *Updated Heat Flow Map of Alaska: Developing a Regional Scale Map for Exploration from Limited Data*. Proceedings from World Geothermal Congress 2015, Melbourne, Australia.

Bronen, R. (2010). *Environment, Forced Migration and Social Vulnerability*. Springer-Verlag Berling Heidelberg, p. 87-98.

Bronin, R. (2013). Brookings-Bern Project on Internal Displacement, *Climate-Induced Displacement of Alaska Native Communities*.

Darrow, M. M. (2011). Thermal Modeling of Roadway Embankments over Permafrost. *Cold Regions Science and Technology, 65*, p. 474-487.

de Grandpré, I., Fortier, D., Stephani, E. (2012). Groundwater flow under transport infrastructure: potential heat flow impacting the thermal regime of permafrost and the degradation of ground ice. *Canadian Journal of Earth Sciences*.

Gibbs, A. E. and Richmond, B. M. (2015). *National Assessment of Shoreline Change – Historical Shoreline Change along the north coast of Alaska, U.S. – Canadian border to Icy Cape: U.S. Geological Survey Open File Report 2015-1048*, 96p. http://dx.doi.org/10.3133/ofr20151048.

Goering, D. J. (2003). Passively Cooled Railway Embankments for use in Permafrost Areas. *Journal of Cold Regions Engineering, 17*(3), p. 119-133.

Johnson, P. R. (1971). *Empirical Heat Transfer Rates of Small Long and Balch Thermal Piles and Thermal Convection Loops*. Institute of Arctic Environmental Engineering, University of Alaska, Report 7102.

Joint Departments of The Army and Air Force, USA. (1988). Technical Manual TM 5-852-6/AFR 88-19, Vol. 6, *Calculation Methods for Determination of Depths of Freeze and Thaw in Soils*, Washington, D.C.

Jorgensen, M. T., and Brown, J. (2005). Classification of the Alaskan Beaufort Sea Coast and estimation of carbon and sediment inputs from coastal erosion. *Geo-Marine Letters*, 25, p. 69-80.

Jorgensen, T., Yoshikawa, K., Kanevskiy, M., and Shur, Y. (2008). *Permafrost Characteristics of Alaska*. Ninth International Conference on Permafrost.

National Oceanic and Atmospheric Administration, U.S. Climate Resilience Toolkit (Last Modified 2015, December). *Relocating Kivalina*. Retrieved from https://toolkit.climate.gov/taking-action/relocating-Kivalina.

National Snow and Ice Data Center. (1998). *Borehole Locations and Permafrost Depths, Alaska, USA, from U.S. Geological Survey*. Retrieved from http://nsidc.org/data/docs/fgdc/ggd223_boreholes.alaska/

Ravens, T. M., Jones, B. M., Zhang, J., Arp, C. D., and Schmutz, J. A. (2012). Process-Based Coastal Erosion Modeling for Drew Point, North Slope, Alaska. *Journal of Waterway, Port, Coastal, and Ocean Engineering*, p. 122-130.

Schaefer, K., Lantuit, H., Romanovsky, V. E., and Schuur, E. A. G. (2012). *Policy Implications of Warming Permafrost*, Nairobi, Kenya, United Nations Environmental Programme Special Report, 50p.

Slusarchuk, W. A., Watson, G. H. (1975). Thermal Conductivity of Some Ice-Rich Permafrost Soils. *Canadian Geotechnical Journal*, 12(3), p. 413-424.

United States Department of Agriculture. (2015). *Barrow (Site 2), Alaska*. Available from http://www.nrcs.usda.gov/wps/portal/nrcs/detail/soils/survey/climate/?cid=NRCS142P2_053693.

United States Environmental Protection Agency. (Last Updated 2016, February). *Climate Impacts in Alaska*. Retrieved: http://www.epa.gov/climatechange/impacts/alaska.html

United States Department of the Interior, Bureau of Land Management. (2009). *Contract No. L09PC00243*.

Urban, F. E., and Clow, G. D. (2014). *DOI/GTN-P Climate and Active Layer Data Acquired in the National Petroleum Reserve – Alaska and the Arctic National Wildlife Refuge, 1998-2013*. Available from http://pubs.usgs.gov/ds/0892/introduction.html.

Wagner, A. (2014). *Review of Thermosyphon Applications, ERDC/CRREL TR-14-1*. The US Army Engineer Research and Development Center.

Western Regional Climate Center. *Barrow WSO Airport, Alaska (500546)*. Available from http://www.wrcc.edu.

Zarling, J. (2011). *Depth of Freeze and Thaw in Soils*. Lecture Notes. University of Alaska, Fairbanks, Alaska.